Journal of Applied Polymer Science

Keratin–Polyhydroxyalkanoate Melt-Compounded Composites with Improved Barrier Properties of Interest in Food Packaging Applications

Pablo Pardo-Ibáñez,[1] Amparo Lopez-Rubio,[1] Marta Martínez-Sanz,[1] Luis Cabedo,[2] José María Lagaron[1]

[1]Novel Materials and Nanotechnology Group, IATA-CSIC), Avenida Agustín Escardino 7, Paterna (Valencia) 46980, Spain
[2]ESID, Universitat Jaume I, Castellón, Spain
Correspondence to: J. M. Lagaron (E-mail: lagaron@iata.csic.es)

ABSTRACT: Sustainable biocomposite materials based on the combination of polyhydroxyalkanoates with a keratin additive derived from poultry feathers were successfully developed via melt compounding. Suitable dispersions for low loadings of the additive in the biopolymeric matrix were achieved by the melt-mixing technique. A good physical interaction between the polymeric matrix and the additive was observed by scanning electron microscopy (SEM). Reductions in water, limonene, and oxygen permeability of the pure polymer to less than a half of its initial value for the composite containing 1 wt % of keratin additive were achieved. This composition was also found to exhibit optimum mechanical performance. As a result, these materials offer significant potential in fully renewable packaging applications based on polyhydroxyalkanoates with enhanced barrier performance. © 2013 Wiley Periodicals, Inc. J. Appl. Polym. Sci. **2014**, *131*, 39947.

KEYWORDS: biopolymers renewable polymers; packaging; thermoplastics

Received 14 May 2013; accepted 27 August 2013
DOI: 10.1002/app.39947

INTRODUCTION

Packaging has developed into an essential technology in the handling and commercialization of foodstuffs to provide the required levels of product quality and safety. In particular, plastic packaging has gained significant importance because of its balanced characteristics (transparency, flexibility, low cost, ease of processing etc.) and the wide variety of formulations that allow the development of packaging structures for specific product requirements.[1] The polymer global market has increased from some 5 million tonnes in the 1950's to more than 100 million tonnes today, the 42% corresponding to the packaging industry.[2] Current research efforts in the area of polymers for food packaging applications are focusing on solving two major drawbacks of these materials. On one hand, the fact that, in contrast to other traditional packaging materials, such as metals, alloys or ceramics,[3] they are not impermeable and, thus, they allow the transport of low molecular weight molecules, such as gases or vapors, which can compromise food quality and safety. On the other hand, the non-renewable origin of most polymers currently used generates strong environmental concerns.

Current strategies to solve these problems include the development of biodegradable polymers obtained from renewable sources, the so-called biopolymers, and their combination with additives to enhance or balance their properties. Amongst the biopolymeric materials that are now attracting more commercial interest, biopolyesters derived from renewable resources, such as polyhydroxyalkanoates (PHAs) and polylactic acid (PLA), present special interest due to their promising properties. These materials can be processed by conventional melt compounding equipment and they are currently being used in a number of applications, particularly in the food packaging and biomedical fields.

PHAs are thermoplastic biopolyesters produced by a variety of bacteria as storage materials in response to particular environmental stresses. Within the PHAs family, the most widely used material is the homopolymer polyhydroxybutyrate (PHB) and its copolymers with hydroxyvalerate (PHBV). Nowadays, the PHAs have become commercially available through many sources and are already being used in small disposable products and in packaging materials.[4] However, many of the commercial products make use of genetically modified organisms (GMOs) as a microbial source and this brings many applicability issues in food packaging. Intense research efforts are currently being dedicated to the production of PHAs based on microbial mixed cultures that make use of by-products as feedstock.[5]

Despite the significant potential of biopolymers to substitute petroleum-based materials helping to reduce environmental impacts, these materials still present a number of property and processing shortcomings that handicap their use in many

applications, particularly in the food packaging field. Specifically, when compared with other traditionally used petroleum-based plastics for food packaging, they present in general lower barrier properties, greater water sensitivity, lower thermal resistance and processing window, lower shelf-life stability due to ageing, migration and a number of other processability issues.[6] In this context, the development of composite materials through the addition of fillers may be an efficient approach to counteract these drawbacks, since thermal, barrier and mechanical properties may be improved without compromising the transparency and toughness, provided that a high dispersion of the filler is achieved. In particular, the use of sustainable additives brings in significant opportunities to develop biobased composite materials with enhanced properties.

Naturally derived proteins from gelatin, soybean, wheat, sunflower, corn, fish, milk, wool, and poultry feathers have been processed into films using a variety of techniques,[7] and some of them have also been used as reinforcement agents in polymeric composites.[8,9] Amongst them, keratin presents special interest because it can be obtained from food by-products like chicken feathers or wool, thus avoiding competence with food products. Keratin is a unique protein because it contains a large amount of the amino acid cysteine compared with other proteins. Cysteine is a sulfur-containing amino acid which can form intra- or intermolecular sulfur–sulfur (S–S) bonds with other cysteine molecules. Intermolecular cysteine bonds, which are referred to as "crosslinks," plus other protein structural features, such as crystallinity and hydrogen-bonding, give keratin high strength and stiffness.[7] In the form of fibers obtained mechanically from poultry feathers, keratin has been added to different polymers not only as a reinforcement[10,11] but also to improve other features such as electrical resistivity[12] and acoustic properties.[13] Despite of this, very few studies are based on the combination of keratin with biopolymers, and no reference has been found dealing with their capacity to modify the gas barrier properties of these matrices. Thus, most of the existing works are focused on developing materials for biomedical applications,[14–16] leaving a wide field of research for the development of biopolymer–keratin composites for food packaging applications.

The main objective of this work was to improve the barrier properties of PHBV matrices through the addition of keratin fibers obtained through the mechanical treatment of poultry feathers, thus developing completely renewable and biodegradable materials and, moreover, making use of a by-product, which has the advantages of being cost-effective and not competing with products aimed for feeding purposes.

EXPERIMENTAL

Materials

The bacterial PHA grade was purchased from Goodfellow Cambridge Limited, United Kingdom, in pellet form (density 1.25 g/cm^3). The supplied material was a melt-processable semicrystalline thermoplastic PHBV12 (polyhydroxybutyrate with 12 mol % of valerate and containing 10 wt % of the plasticizer citric ester) copolymer made by biological fermentation from renewable carbohydrate feedstocks.

Poultry feathers were kindly supplied by Mayava. S.L. (Valencia, Spain). Feathers were first sanitized with a bath in ethanol (96%), 1:2 feathers to ethanol ratio in mass, followed with a second bath in ethanol (70%) using the same ratio. Afterwards, feathers were dried overnight at 50 C.

Keratin Additive Preparation

Keratin additive was obtained by grinding the poultry feathers using a two-step procedure previously described in a patent application.[17] Feathers were first ground in a rotational-blade comminuting machine Fitz Mill Model D equipped with a 3-mm sieve. Blades rotated at a constant speed, cutting the feathers and pushing them through the sieve. The passing product was then collected in a container. Feathers were slowly added to avoid overheating of the system.

The product obtained after this first step was then milled in a Fritsch Pulverisette 9 vibrating cup mill, using a milling set of 100-mL cup, ring and cylinder of tungsten carbide-coated stainless steel. The cup containing the sample together with the ring and the cylinder rotated at 1600 rpm in an eccentric trajectory applying high impact and shear stress to the material. Loads of 4 g of ground feathers were treated for 1 min in intervals of 10 s separated by pauses of the same duration to avoid overheating the sample. A loose powder with the particle size distribution presented in Figure 1 was obtained.

Particle Size Analysis

Particle size distribution was determined by laser diffractometry using a Malvern Mastersizer 2000 equipped with a low-volume wet dispersion unit. Measurements were performed in aqueous dispersion.

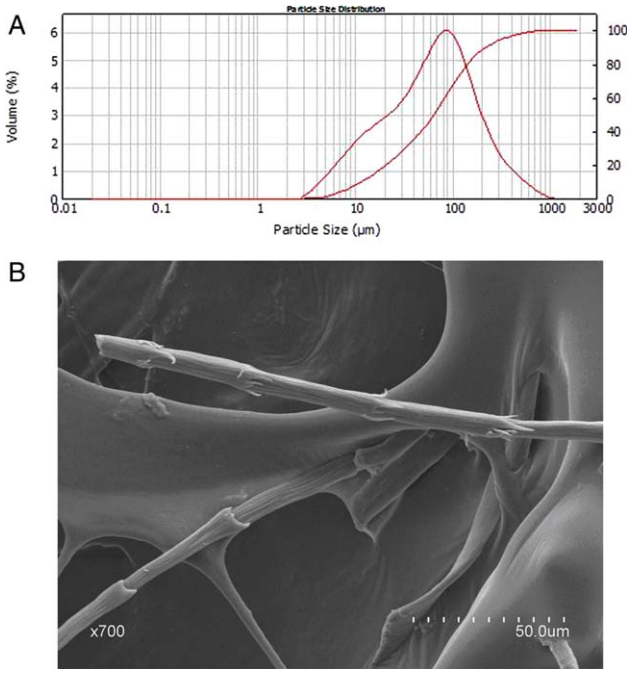

Figure 1. Particle size distribution (A) and SEM micrograph (B) of the keratin additive. [Color figure can be viewed in the online issue, which is available at wileyonlinelibrary.com.]

Preparation of Composite Materials

Different weight percentages of keratin powder obtained as previously described were dispersed in PHBV12 by melt-mixing in a Brabender Plastograph mixer (16 cm^3) for 4 min at 160°C. Keratin additions ranged from 0 to 50% by weight of PHBV12. The mixing temperature was chosen low enough to avoid excessive thermal exposure of the keratin but high enough to melt PHBV12. Keratin was mixed with the polymer pellets and, then, both components were added together to the mixer. After mixing, the batches were left at room temperature to cool-down.

Film Conformation

Aliquots of ca. 0.3 g of the blends of PHBV with the mechanically treated feathers were sandwiched between glass fiber reinforced PTFE foils using a 25 cm^2 template of the same material. A pressure of 58 MPa was applied for 4 min at 165°C using a Carver hot-plate hydraulic press.

Optical Microscopy

Polarized light microscopy (PLM) examinations were performed using a Nikon Eclipse 90i optical microscope (IZASA, Spain) equipped with a 5-megapixels cooled digital color microphotography camera Nikon Digital Sight DS-5Mc. Captured images were analyzed and processed by using Nis-Elements BR software.

Measurement of Transparency

The transparency of films was determined from their surface reflectance spectra as described in a previous work.[18] A spectrophotometer KONICA MINOLTA CM-2600d was used to perform measurements on a black and white background in triplicate for each sample. Kubelka-Munk theory for multiple scattering[19] was applied to the reflection spectra for the determination of the transparency. Internal transmittance T_i in the films was quantified by applying Eq. (1)[20] where R_0 is the reflectance of the layer with an ideal black background and R_g is the reflectance of the sample layer backed by a known reflectance.

$$T_i = \sqrt{(a - R_0)^2 - b^2} \tag{1}$$

$$a = \frac{1}{2}\left(R + \frac{R_0 - R + R_g}{R_0 \cdot R_g}\right) \tag{2}$$

$$b = \left(a^2 - 1\right)^{1/2} \tag{3}$$

Scanning Electron Microscopy (SEM)

For SEM observation, the samples were cryofractured after immersion in liquid nitrogen, mounted on bevel sample holders and sputtered with Au/Pd under vacuum. Micrographs of the fracture surface were taken with a Hitachi S4800 scanning electron microscope, working with an accelerating voltage of 5 kV.

Gravimetric Measurements

Direct permeability to D(+)-limonene of 95% purity (Panreac Química, Spain) at 60%RH in the outer atmosphere and direct permeability to water at 0%RH in the outer atmosphere were determined from the slope of weight loss vs. time curves at 24°C. The films were sandwiched between the aluminum top (open O-ring) and bottom (deposit for the permeant) parts of aluminum permeability cells with the help of a Viton rubber O-ring to enhance sealability. The deposit was filled with the permeant and the pinhole secured with three screws. Finally, the cells were placed in the desired environment (0%RH desiccator for water measurements and chamber conditioned at ~60% RH and 25°C for limonene testing) and the solvent weight loss through a film area of 0.001 m^2 was monitored and plotted as a function of time. Cells with aluminum films (with thickness of ca. 100 microns) were used as control samples to estimate solvent loss through the sealing. Cells clamping polymer films but with no solvent were used as blank samples to monitor water uptake. Solvent permeation rates were estimated from the steady-state permeation slopes, i.e., only the linear part of the weight loss data was used. Water vapor weight loss was calculated as the total cell loss minus the loss through the sealing. Organic vapor weight loss was calculated as the total cell loss minus the loss through the sealing and plus the water weight gain. The tests were done in triplicate for both permeants.

Oxygen Transmission Rate

The oxygen permeability coefficient (P) was derived from oxygen transmission rate (OTR) measurements recorded using an Oxtran 100 equipment (Modern Control, Minneapolis, MN). The temperature was kept at 24°C, while experiments were performed at 80% RH, generated by a built-in gas bubbler and checked with a hygrometer placed at the exit of the detector. Experiments were done in duplicate. Samples were purged with nitrogen for a minimum of 20 h, prior to exposure to a 100% oxygen flow of 10 mL/min, and a 5 cm^2 sample area was measured by using an in-house developed mask.

Differential Scanning Calorimetry

Differential scanning calorimetry (DSC) of PHBV and its composites was performed on a Perkin-Elmer DSC 7 thermal analysis system on typically 7 mg of material at a scanning speed of 10°C/min. Two heating scans were carried out from −40°C to 170°C separated with a cooling scan at the same rate. The baseline of the thermograms was corrected with similar runs of an empty pan and the DSC equipment was calibrated with an indium standard.

Crystallinity was estimated using the ratio between the heat of fusion of the studied material and the heat of fusion of a perfect crystal of same material, i.e.,

$$\%X_c = \frac{\Delta H_f}{\Delta H_f^0} \times 100 \tag{4}$$

where ΔH_f is the enthalpy of fusion of the studied specimen and ΔH_f^0 is the enthalpy of fusion of a totally crystalline material ($\Delta H_f^0 = 146$ J/g for PHBV[21]).

Mechanical Properties

Tensile tests were carried out at 24°C and 50% RH on an Instron 4400 Universal Tester. Dumb-bell shaped specimens with initial gauge length of 25 mm and 5 mm in width were die-stamped from the sheets in the machine direction according to ASTM standard method D882[22]). The thickness of all specimens was approximately 100 μm. A fixed crosshead rate of 10 mm/min was utilized in all cases, and results were taken as the average of four tests. The samples were preconditioned at 54% RH before testing and were assayed within 2 weeks after preparation of the films.

Modeling of the mechanical properties using the Halpin-Tsai equation [eq. (5)] was carried out to compare the experimental results with the theoretical expectations.[23]

$$E=\frac{E_m(1+\xi\eta\varphi)}{1-\eta\varphi} \quad (5)$$

where

$$\eta=\frac{\frac{E_r}{E_m}-1}{\frac{E_r}{E_m}-\xi} \quad (6)$$

$$\xi=\frac{2\times \text{length}}{\text{thickness}} \quad (7)$$

E_r and E_m refer to the Young's modulus of the matrix and the reinforcement, respectively, and φ is the volume fraction of the additive. For the calculations, E_m was experimentally determined ($E_{PHBV12} = 670.31$ MPa) and E_r was consulted in the existing bibliography ($E_{\text{chicken feather fiber}} = 3590$ MPa[24]).

Statistical Analysis

One-way analysis of the variance (ANOVA) was performed using Statgraphics 5.1 software package. Comparisons between samples were evaluated using the Tukey test.

RESULTS AND DISCUSSION

Morphology, Dispersion, and Optical Properties of PHBV-Based Composite Films

In this work, a keratin additive was produced by mechanical treatment of chicken feathers. The morphology of the produced filler was studied by particle size analysis and SEM. Figure 1(A) shows the cumulative and frequency curves of the particle size distribution of the keratin additive. Although the total range of the distribution was wide, 70% of the volume of the sample was less than 100 μm. From the results, the estimated average particle length was ca. 30 μm and the absolute maximum of frequency corresponded to 80 μm. On the other hand, SEM observations confirmed that keratin particles presented fibrillar morphology, in accordance with a previous work,[25] with a rather uniform diameter of 5 μm [cf. Figure 1(B)]. Considering this, the average aspect ratio, i.e., length to diameter, of the fibers was 6, with a main population of fibers with an aspect ratio of 16.

This keratin additive was subsequently incorporated into PHBV12 by melt compounding and composite films were prepared by compression moulding. Figure 2 shows the contact transparency images of the biocomposite films with different keratin loadings. It can be observed that the transparency of the pure PHBV12 was kept for the films containing up to 5 wt % of keratin additive. A yellowish coloration caused by the keratin was noticeable from 3 wt % of additive, increasing gradually with its addition percentage. Films with percentages of additive over 10 wt % presented a noticeable loss in transparency and higher coloration effect. It is known that chicken feather fibers present a thermal degradation profile which comprises a first degradation step ranging from 265°C to 350°C corresponding to the protein denaturation, followed by a second decomposition step from 350°C onwards.[26,27] Thus, suggesting that this yellowish color was not caused by thermal degradation of the filler during melt processing.

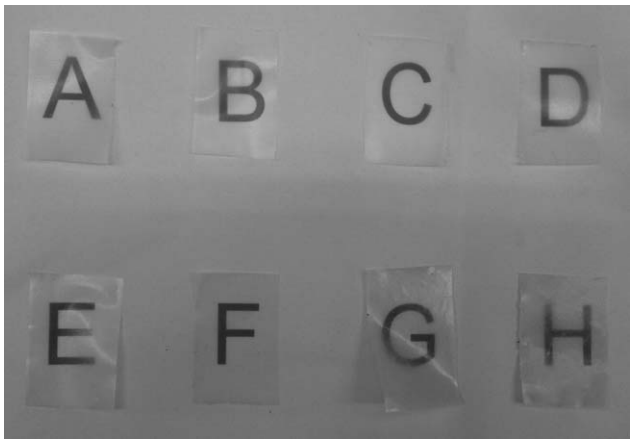

Figure 2. Photographs of PHBV films containing 0 wt % (A), 0.5 wt % (B), 1 wt % (C), 3 wt % (D), 5 wt % (E), 10 wt % (F), 25 wt % (G), and 50 wt % (H) of keratin.

Film transparency was evaluated through the variation of the internal transmittance (T_i) values and the results are shown in Figure 3. A decrease in these values implies higher opacity of the materials, while increasing values can be related to more homogeneous and transparent films. The sample without keratin additive showed the highest values of T_i, and a gradual decrease of these parameters was observed as the amount of additive increased. In agreement with the previous contact transparency images, it can be concluded that the transparency of the pure PHBV12 was preserved for samples with loadings up to 3–5 wt %. In contrast, the sample with 50 wt % of keratin additive showed the maximum drop in the transparency with a reduction of 20% to 10% of T_i over the wavelength range studied.

The morphology of the generated biocomposites was studied by optical microscopy and SEM. Figure 4 shows representative optical microscopy images corresponding to the samples loaded

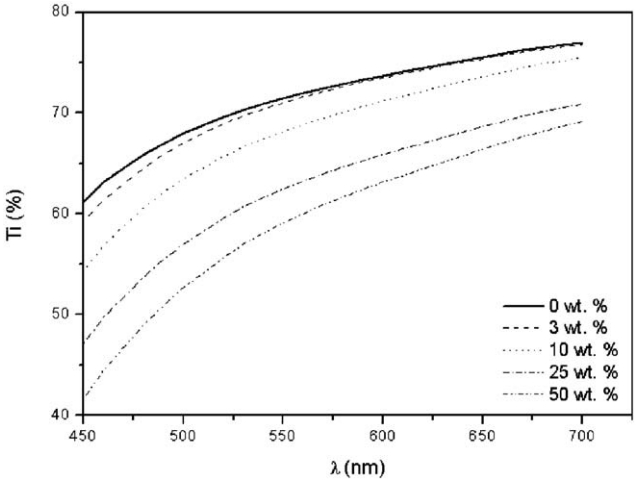

Figure 3. Spectral distribution of internal transmittance (T_i) of control and films with different additive loadings.

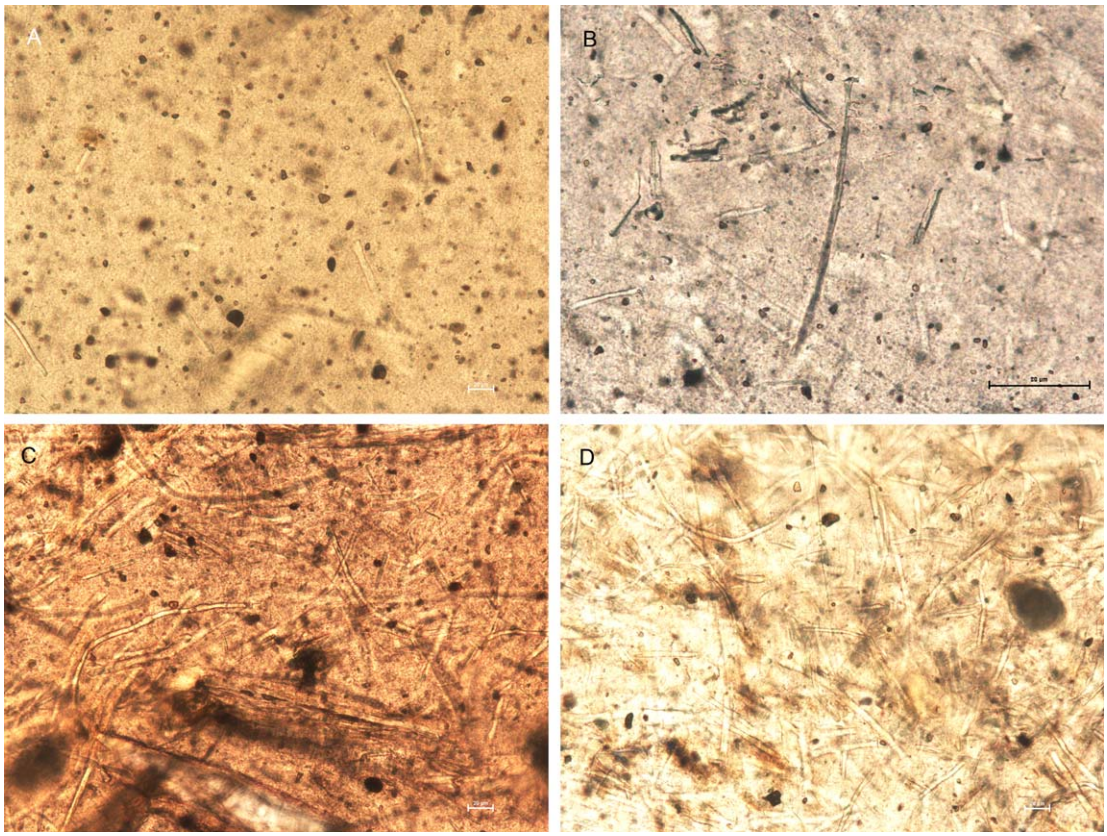

Figure 4. Optical microscopy images of PHBV films containing 1 wt % (A), 5 wt % (B), 10 wt % (C), and 25 wt % (D) of keratin additive. Scale bar corresponds to 20 μm for A, C, and D and to 30 μm for B. [Color figure can be viewed in the online issue, which is available at wileyonlinelibrary.com.]

with 1, 5, 10, and 25 wt % of additive. The keratin additive was identified as fibers of different sizes. Aggregation of fibers was observed in the materials with additive loadings higher than 5 wt %, which is also in agreement with the reduced transparency observed for these samples. This poor dispersion departs from the ideal scenario in which individual particles with good adhesion to the polymeric matrix influence the free volume on the surrounding region and increase the tortuosity of the diffusion path that the permeate needs to follow across the material, both effects decreasing the permeability of the composite.[28] Therefore, a barrier decrease could be expected for loadings higher than 5 wt %.

Figure 5 presents representative SEM images of cryofractured sections of the biocomposite films. The elongated shape of the fibers discussed above, with their relatively high aspect ratio, favored an arrangement in which fibers were randomly distributed but oriented with their length parallel to the film surfaces. Images 5A and 5B, corresponding to films with 1 and 5 wt % additive respectively, confirm that keratin fibers were homogeneously dispersed through the film thickness, showing a fairly good adhesion to the polymer matrix [cf. Figure 5(C,D)]. Poor dispersion and aggregation of fibers was observed for higher contents of additive, supporting the previous optical microscopy observations. Concerning the fracture process, there were some fiber pullouts, as noticed by the exposed fibers. Nevertheless, the fiber fragments were not very long, and some were fractured in the same fracture plane as the polymer [cf. Figure 5(C), left side], indicating strong fiber/polymer interactions. A similar morphology and matrix–filler adhesion was observed for PLA composites loaded with chicken feather fibers prepared by extrusion,[26] although in that case most of the fibers were broken off together with the PLA matrix, suggesting that the keratin fibers present improved adhesion with a PLA matrix as compared with the PHBV used through this work. In any case, it seems that the keratin fillers present a relatively good compatibility with hydrophobic polymers. This interaction was helped by the intrinsic surface roughness of the fibers [cf. Figures 5(C,D)], which increases the surface area by a factor of about 2.2 over a perfectly smooth fiber.[25]

Thermal Analysis

Thermal properties of the composite materials were evaluated by means of DSC analyses. The melting temperature (T_m) and heat of fusion (ΔH_m) were determined from the first and second heating runs. The degree of crystallinity (X_c) of the composites was determined from the first heating run curve, which offers information related to the thermal characteristics of the obtained material, just after its preparation. Crystallization temperature (T_c) was also measured on the cooling run.

Multiple melting peak behavior of PHBV copolymers was interpreted previously[29] as an effect of the melting-recrystallization process occurring during subsequent heating. From the data

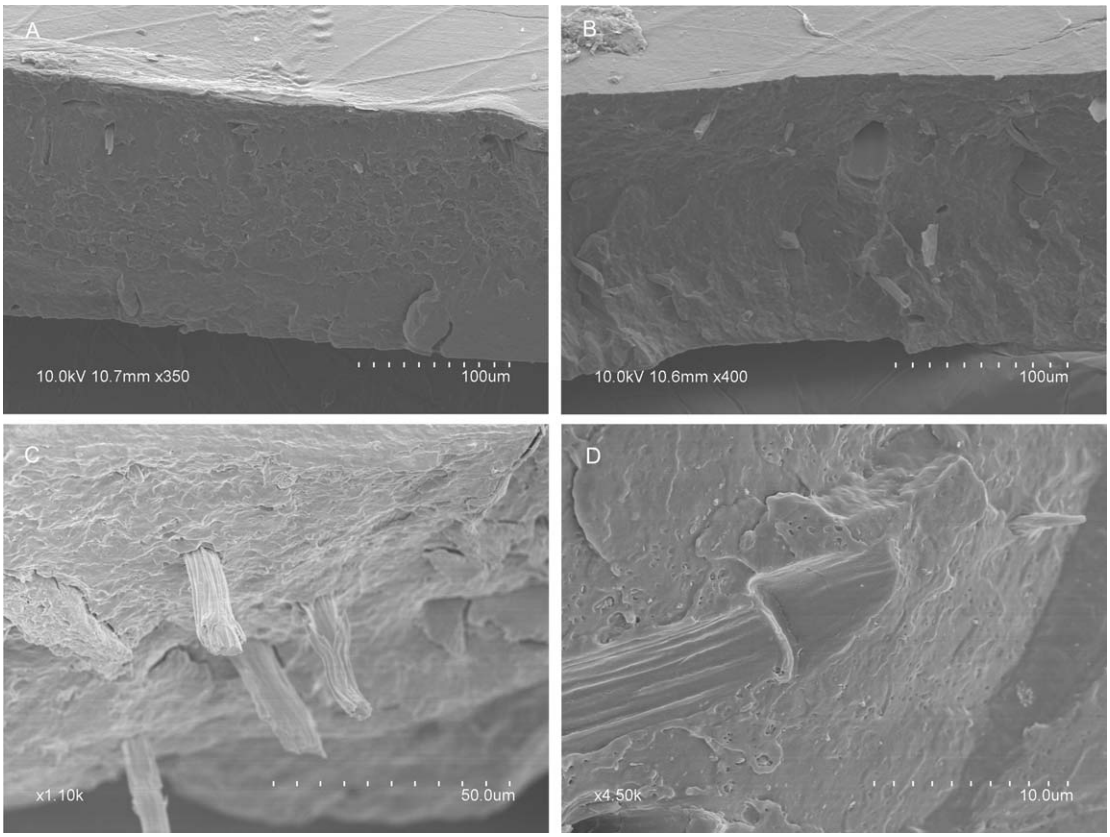

Figure 5. SEM micrographs of the cryofractured section of PHBV films containing 1 wt % (A and C) and 5 wt % of keratin additive (B and D).

gathered in Table I it can be observed that the melting point was not affected or just showed slight variations along the whole range of additions for both heating runs. This observation is in agreement with previous results on the production of PLA composites containing keratin fibers[26] and discards severe filler-induced polymer degradation phenomena, which has been reported for PHBV composites containing nanoclays.[30] The crystallization temperature also remained unmodified or with no significant variations for all the studied addition percentages. In contrast, for up to 3 wt % of keratin addition, crystallinity was not modified or slightly increased, whereas greater additive contents led to a drop in the crystallinity value, indicating that the presence of greater keratin fiber contents hindered significantly the crystallization process. This result is again related to the fact that loadings higher than 3–5 wt % resulted in significant agglomeration of the filler, therefore distorting the crystalline network of the pure PHBV12. Therefore, it is expected that the agglomeration observed for composites with high contents of keratin fibers may have an impact on the barrier properties of the materials as a result of the reduced crystallinity, as crystallites are considered to be impermeable to the passage of low molecular weight molecules.

Mass Transport Properties

Table II summarizes the water, limonene and oxygen permeability coefficients for the pristine melt mixed PHBV12 and its composites with 0.5, 1, 3, 5, 10, 25, and 50 wt % of keratin. Regarding water permeability, an optimum additive percentage was observed at 1 wt % keratin addition, resulting in a permeability reduction of 59%. The rest of the compositions showed no significant effect on the water barrier, except for filler loadings higher than 5 wt %, where noticeable barrier losses were seen, although due to the variability of data statistically significant differences were only found for loadings higher than 25 wt %. When limonene was considered as the permeant, a similar behavior was observed. The composite material containing 1 wt % of keratin presented a significant reduction of 55% in the permeability, whereas, similarly to what was found with water, a detrimental effect in the limonene barrier properties was observed for composites containing more than 5 wt % of the filler, but again statistically significant differences were found only for the composite with 50 wt % of the keratin filler as a result of the large data variability. Regarding the oxygen permeability, the greatest reduction, of ca. 67% as compared with the pure polymer, was also found for the 1 wt % keratin composite. A slight improvement in the oxygen barrier properties, in comparison with the pure PHBV, was also observed for the samples containing 3 wt % keratin but, as observed from Table II, higher loadings did not lead to an improvement in the oxygen barrier properties, with excessive OTRs for additions beyond 5 wt %. This result is in agreement with a previous work in which low density polyethylene composites loaded with 5 wt % and 10 wt % chicken feathers were produced, observing a significant increase in the oxygen permeability with the addition of the

Table I. DSC Melting Point (T_m), Melting Enthalpy (ΔH_m), Degree of Crystallinity (X_C) and Crystallization Temperature (T_C) of Melt Mixed PHBV12 and Its Composites with 0.5, 1, 3, 5, 10, 25, and 50 wt % of Keratin Fibers

Sample	1st heating T_m (°C)	1st heating ΔH_m (J/g)	1st heating % X_C	2nd heating T_m (°C)	2nd heating ΔH_m (J/g)	T_c (°C)
0% Keratin	139.4-153.4 ± (0.3-0.1)	37.7 ± 0.9	26.0 ± 1.3	147.9-157.0 ± (0.1-0.4)	46.0 ± 7.0	103.0 ± 0.0
0.5% Keratin	138.9-152.7 ± (0.8-0.3)	38.0 ± 5.0	26.0 ± 4.0	147.6-156.7 ± (1.1-0.9)	49.0 ± 12.0	102.4 ± 1.4
1% Keratin	138.2-152.8 ± (0.1-0.0)	37.8 ± 0.4	26.0 ± 0.6	147.5-156.7 ± (0.2-0.5)	46.0 ± 3.0	103.3 ± 0.5
3% Keratin	139.8-153.0 ± (0.1-0.2)	39.0 ± 2.0	26.8 ± 0.0	147.1-156.4 ± (0.3-0.5)	45.0 ± 4.0	102.1 ± 0.1
5% Keratin	141.2-153.2 ± (0.2-0.7)	26.2 ± 1.3	18.0 ± 0.6	148.3-157.3 ± (1.8-1.8)	43.0 ± 6.0	103.3 ± 1.6
10% Keratin	136.2-152.5 ± (0.1-0.2)	31.0 ± 2.0	21.0 ± 0.6	147.1-156.5 ± (0.4-0.5)	44.0 ± 10.0	101.9 ± 0.3
25% Keratin	142.3-153.4 ± (0.7-0.1)	29.3 ± 1.5	20.1 ± 2.0	147.4-156.7 ± (0.3-0.2)	49.9 ± 11.2	102.5 ± 1.3
50% Keratin	139.6-153.0 ± (0.6-0.1)	24.2 ± 1.1	16.6 ± 1.5	147.3-156.3 ± (0.8-0.6)	35.0 ± 11.0	102.0 ± 0.9

filler,[31] thus confirming that only low loadings may improve the oxygen barrier properties. The existence of an optimum in the dispersion of the additive, corresponding to low addition percentages, specifically to 1 wt %, could justify the reduction in permeability of this specific composite material observed for the three different permeant substances studied. An optimum dispersion, where particles are not aggregated but homogeneously distributed within the polymeric matrix is thought to increase the tortuosity in the diffusion path of the permeant, thus reducing the permeability. Depending on the chemical nature of the additive and the particle size and shape this optimum percentage can vary. As an example, optimal barrier properties have been reported previously in PHBV reinforced with 5 wt % clay nanoparticles.[30] Moreover, it is clear that keratin loadings greater than 5 wt % are detrimental for the barrier properties of the composite materials, as one the one hand, there is significant filler agglomeration and on the other hand, the crystallinity of the material is decreased, just as pointed out by DSC results.

It should also be mentioned that filler-induced polymer hydrolysis, which is commonly associated with the melt-mixing process,[32] seems to take place to a certain extent, as suggested by the lower barrier performance of the pure polymer if compared with the same material when processed by the solution casting technique.[33] However, filler addition did not seem to further promote polymer hydrolysis, as deduced from the thermal characteristics of the composite biomaterials obtained in this work. In addition, the permeability values can also be affected by the presence of plasticizers, the mixing and conformation procedures and the thermal history of the material, among other factors. As indicated by the distributor, the PHBV used in this work contained a 10 wt % of citric ester as plasticizer. In a review on the main physical properties of different commercial PHAs,[34] an increase in the oxygen permeability of some of the studied biopolyesters due to the presence of plasticizers was reported. Therefore, the values provided in Table II are comparable within the set of samples, but a comparison in absolute terms with determinations made on other PHAs can be difficult to establish.

Table II. Water, Limonene and Oxygen Permeability Coefficients for PHBV12 and Its Composites with 0.5, 1, 3, 5, 10, 25, and 50 wt % of Keratin Fibers

Sample	Water permeability ($\times 10^{-15}$) (kg m/s m^2 Pa)	Limonene permeability ($\times 10^{-15}$) (kg m/s m^2 Pa)	80% RH Oxygen permeability ($\times 10^{-18}$) (m^3 m/(m^2 s Pa))
0% Keratin	7.4 ± 0.6^{ab}	8.3 ± 1.1^{a}	3.0 ± 0.1^{b}
0.5% Keratin	7.8 ± 0.3^{ab}	9.0 ± 2.6^{a}	3.1 ± 0.4^{b}
1% Keratin	3.1 ± 0.0^{a}	3.7 ± 0.3^{a}	1.0 ± 0.2^{a}
3% Keratin	7.9 ± 0.4^{ab}	8.3 ± 0.5^{a}	2.6 ± 0.1^{b}
5% Keratin	7.4 ± 0.6^{ab}	8.4 ± 0.6^{a}	3.2 ± 0.5^{b}
10% Keratin	9.0 ± 2.0^{ab}	9.5 ± 5.3^{a}	-
25% Keratin	20.0 ± 2.0^{b}	8.0 ± 1.1^{a}	-
50% Keratin	62.0 ± 16.0^{c}	22.7 ± 2.3^{b}	-
PHBV12 casting[33]	1.3 ± 0.1*	1.3 ± 0.1*;	1.4 ± 0.0

The a, b and c letters correspond to the ANOVA statistical analysis and Tukey test of the data that indicate that with a 95% confidence level, the values are significantly different.
*Measured at 40% RH.

It is also interesting to note that whereas for the pure PHBV the permeability to the three different permeants was such that $P_{limonene} > P_{H2O} > P_{O2}$, when increasing the filler content over 25 wt % the water permeability became higher than the limonene permeability. This observation may suggest that, while the pure polymer presented higher affinity for the less polar limonene, when incorporating the keratin filler, with its amphiphilic nature, the overall hydrophilic character of the material was increased and as a result water permeability was affected to a higher extent than limonene permeability by the addition of the filler.

An additional assessment of the barrier performance was carried out by comparing the experimental data with the results obtained when applying a theoretical model. Maxwell[35] developed a model to describe the conductivity of a two-phase system in which permeable spheres P_d are dispersed in a continuous permeable matrix P_m. Fricke[36] extended Maxwell's model to consider the conductivity of a system consisting in ellipsoids of permeability P_d dispersed in a more permeable continuous matrix. Equation (7) describes the permeability of the composite system[37]:

$$p = \frac{(p_m + P_d F)}{(1+F)} \tag{8}$$

where

$$F = \left[\frac{\varphi_2}{1+\varphi_2}\right]\left[\frac{1}{1+(1-M)\left(\frac{P_d}{P_m}-1\right)}\right] \tag{9}$$

$$M = \frac{\mathrm{Cos}\theta}{\mathrm{Sin}^3\theta}\left[\theta - \frac{1}{2}\sin 2\theta\right] \tag{10}$$

$$\cos\theta = \frac{W}{L} \tag{11}$$

$$\varphi_2 = \frac{W_r/\rho_r}{W_r/\rho_r + \frac{1-W_r}{\rho m}} \tag{12}$$

Being W the dimension of the axis of the ellipsoid parallel to the direction of transport and L the dimension of the axis perpendicular to the direction of transport, with θ in radians, and φ_2 the volume fraction of the reinforcement, calculated from the weight fraction of the reinforcement w_r and the density of the reinforcement and the matrix, ρ_r and ρ_m, respectively. This model approaches the Maxwell model as the L/W ratio trends to unity.

Figure 6 shows the relative variation in permeability calculated using Fricke's model for L/W ratios of 6, 16, and 500, considering $P_m = 100$ and $P_d = 1$[38], $\rho_r = 0.89$ g/cm^3,[11] and $\rho_m = 1.25$ g/cm^3, together with the normalized variation in permeability to water vapor, limonene, and oxygen of the samples. The variation in permeability measured for the samples oscillated over and under the model plots, indicating that, due to the nature of the additive, its behavior was not well described by these models. Keratin reinforcement presented a wide particle size distribution as determined by laser diffractometry. This implies a wide distribution of aspect ratios, a circumstance which was not considered in the application of the Fricke's model, with the consequent mismatch between the measured values and the modeling. For the samples with the higher percentages of addition, aggregation phenomena discussed above implied an additional deviation from the assumptions of the model, resulting in a greater disagreement between the predicted and experimental values. Considering the composition with the maximum decrease of permeability for the three permeants, i.e., 1 wt % keratin additive, it would correspond to an effective aspect ratio of over 500 according to the theoretical model, which is much greater than the experimental average aspect ratio of 6. This underestimation of the filler blocking capacity has been previously detected for different systems, as for example PLA and EVOH nanocomposites loaded with highly dispersed cellulose nanowhiskers[39,40] and it was explained by the fact that aside from the diffusion reduction caused by the greater tortuosity produced with low filler loadings, other phenomena such matrix morphological alterations and reduced sorption of the permeant were also taking place and contributing to the permeability drop.

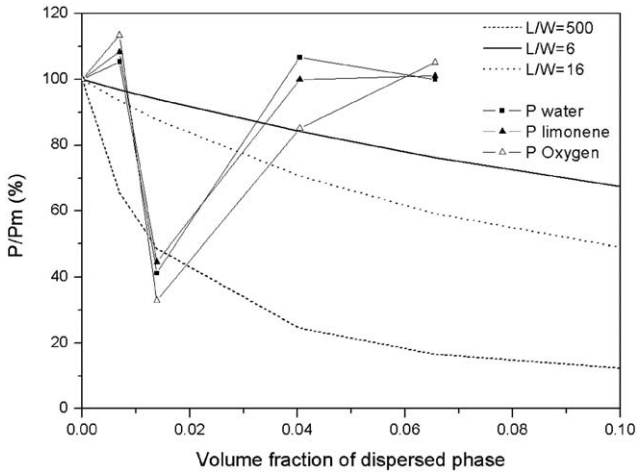

Figure 6. Relative permeability (P/P_m) versus volume fraction of dispersed phase modelled with different aspect ratios L/W and the normalized experimental permeability values for water vapor, limonene, and oxygen.

Mechanical Properties

Figure 7(A) shows the dependence of the elastic modulus and elongation at break with the keratin additive loading. For additions of 1 and 3 wt % a significant increase in elastic modulus of ca. 30% and 20% respectively, over the pure PHBV was observed. This increase has been also observed in LDPE at low loadings of a similar keratin reinforcement.[11] Under this finding and supported by microscopy observations, the authors reported an interaction between the reinforcement and the polymer without the need for coupling agents or chemical treatment of the fibers. On the other hand, it is clearly observed that upon increasing the filler loading there was a drop on the elastic modulus. This later fact may be related to the filler agglomeration observed for higher keratin loadings. The elongation at break [cf. Figure 7(B)] decreased with the keratin content of the composites, evidencing a loss in ductility for the films. Thus, low additive contents, up to 1 wt %, should be incorporated to limit the brittleness increase of the composite materials. In particular, a composition of 1 wt % filler yielded the combination of the lowest permeability and the highest elastic modulus, with an acceptable ductility drop as compared with the pure biopolymer.

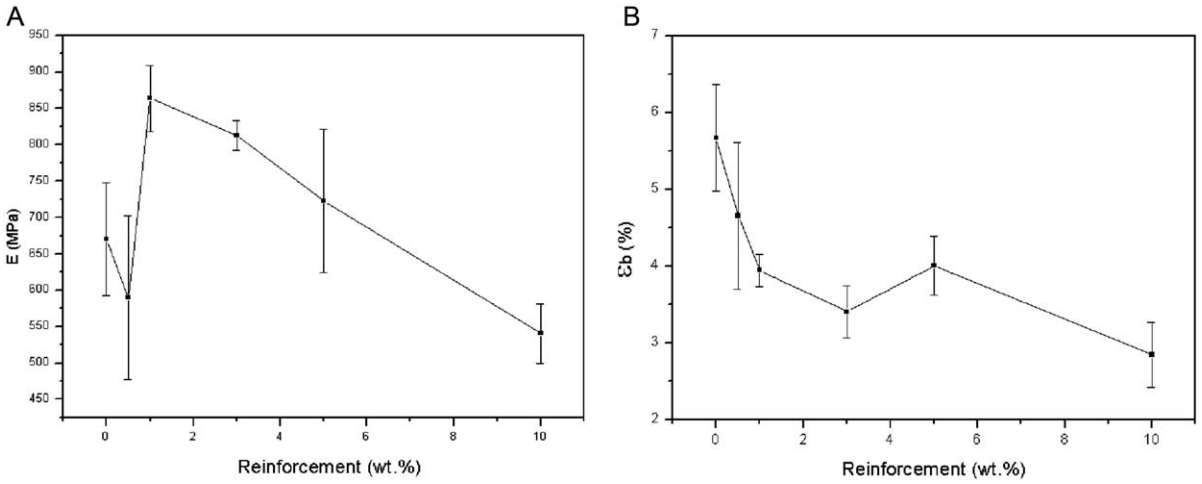

Figure 7. Elastic modulus (A) and elongation at break (B) of the PHBV composite films for the different additive loadings.

A previous study in which PLA composites loaded with chicken feather fibers were developed,[26] reported reductions in the tensile strength for all the composite samples and increased elongation at break for filler loadings up to 5 wt %, while the elastic modulus was not significantly affected. Thus, chicken feathers showed a plasticizing effect in that case, in contrast with the ductility drop observed in this work. This different effect may be explained by an enhanced matrix–filler adhesion observed for the PLA composites, as already pointed out by the morphological analyses.

As detailed in the materials and methods section, modeling of the experimental mechanical properties using the Halpin-Tsai equation, to compare them with the theoretical expectations, was performed. As previously reported, a fiber thickness of 5 μm was considered together with the mean length ($D[3,2] = 30.3$ μm). The value of the maximum of the frequency distribution of lengths, 80 μm, was also considered in a second calculation.

Figure 8 shows the comparison between the theoretical results for both lengths considered and the experimental values. As previously observed with the permeability evolution, theoretical models did not match the experimental results, underestimating the increase in Young's modulus found for composites with 1 wt % and 3 wt % additions. Once again, the wide particle size distribution of the additive, generating a wide range of aspect ratios which was not considered in the model, together with the poor dispersion and aggregation of additive fibers in highly loaded samples would be the main reasons of the observed discrepancy between experimental and theoretical results.

Measurements of samples of the higher loaded compositions performed with the methodology described were poorly reproducible and were not considered for discussion.

CONCLUSIONS

Novel biodegradable and renewable composite materials based on the combination of PHAs with a keratin additive prepared from poultry feathers were successfully developed. Suitable dispersion for low loadings of the additive in the biopolymeric matrix was achieved by melt mixing. This good dispersion led to barely unmodified optical properties for the obtained films. Although chemical interaction between the keratin additive and the polymer did not take place, a good physical adhesion was observed by SEM. The combination of this adhesion and the adequate dispersion of the additive enhanced the barrier properties of the pure polymer, reducing its water, limonene and oxygen permeability to less than a half of its initial value for the composite containing 1 wt % of keratin additive. This composition was found to be the optimum not only in the improvement of barrier properties but also when mechanical properties were considered. An increase of ca. 30% over the pristine polymer in the elastic modulus was found for this addition percentage. In contrast, samples containing more than 10 wt % keratin fibers presented poor optical properties and high permeability values.

The increased barrier properties of the 1 wt % addition biocomposite to water, limonene, and oxygen, and its enhanced elastic modulus, made this specific composite a suitable

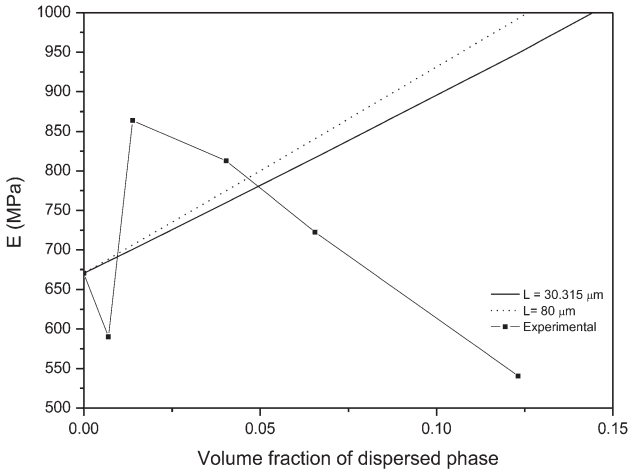

Figure 8. Comparison between theoretical predictions by Halpin-Tsai method and experimental values of Young's modulus for the different composites.

candidate for the development of biodegradable non-petroleum based food packaging material. On the other hand, considering the upper end of the studied range of additions, biocomposites with high percentages of additive can be of use in specific packaging applications where the exchange of gases and/or water vapor is needed, regardless of transparency.

ACKNOWLEDGMENTS

A. Lopez-Rubio is the recipient of a "Ramon y Cajal" contract from the Spanish Ministry of Economy and Competitivity. M. Martínez-Sanz thank the Spanish Ministry of Education for the FPU grant. The authors acknowledge financial support from MICINN (MAT2009-14533-C02-01 project) and the EU FP7 ECOBIOCAP project. The SCIE from the University of Valencia is acknowledged for the support with SEM analysis.

REFERENCES

1. Lagarón, J. M.; Cabedo, L.; Cava, D.; Feijoo, J. L.; Gavara R.; Gimenez E. *Food Addit. Contam.* **2005**, *22*, 994.
2. Silvestre, C.; Duraccio, D.; Cimmino, S. *Prog. Polym. Sci.* **2011**, *36*, 1766.
3. López-Rubio, A.; Hernández-Muñoz, P.; Catala, R.; Gavara, R.; Lagarón, J. M. *Food Addit. Contam.* **2005**, *22*, 988.
4. Sánchez-García, M. D.; Gimenez, E.; Lagarón J. M. *Carbohydr. Polym.* **2008**, *71*, 235.
5. Akaraonye, E.; Keshavarz, T.; Roy, I. *J Chem Technol Biotechnol.* **2010**, *85*, 732.
6. Hauggaard, V. K.; Udsen, A. M.; Mortensen, G.; Hoegh, L.; Petersen, K.; Monahan F. In Food Biopackaging, in Biobased Packaging Materials for the Food Industry—Status and Perspectives; Weber, C. J., Ed.; A European concerted action: Copenhagen, Denmark, **2001**, pp. 13–14.
7. Barone, J. R.; Schmidt, W. F.; Liebner, C. F. E. *J. Appl. Polym. Sci.* **2005**, *97*, 1644.
8. Sionkowska, A. *Prog. Polym. Sci.* **2011**, *36*, 1254.
9. Barone, J. R. *J. Polym. Environ.* **2009**, *17*, 143.
10. Saucedo-Rivalcoba, V.; Martínez-Hernández, A. L.; Martínez-Barrera, G.; Velasco-Santos, C.; Castaño, V. M. *Appl. Phys. A: Matter* **2011**, *104*, 219.
11. Barone, J. R.; Schmidt W. F. *Compos. Sci. Technol.* **2005**, *65*, 173.
12. Zhan, M.; Wool, R. P.; Xiao J. Q. *Compos. Part A: Appl. S.* **2011**, *42*, 229.
13. Huda, S.; Yang, Y. *J. Polym. Environ.* **2009**, *17*, 131.
14. Lam, P. M.; Lau, K. T.; Zhao, Y. Q.; Cheng, S.; Liu, T. 17th International Conference on Composite Materials, **2009**.
15. Cheng, S.; Lau, K.; Liu, T.; Zhao, Y.; Lam, P. M.; Yansheng Y. *Compos. Part B: Eng.* **2009**, *40*, 650.
16. Tanabe, T.; Okitsu, N.; Tachibana, A.; Yamauchi, K. *Biomaterials* **2002**, *23*, 817.
17. Lagarón, J. M.; Pardo, P.; Lopez-Rubio, A.; (Consejo Superior de Investigaciones Científicas, CSIC) Spain Pat. P201231146, July *19*, **2012**.
18. Fabra, M. J.; Talens, P.; Chiralt, A. *Food Hydrocolloids.* **2009**, *23*, 676.
19. Hutchings, J. B. In Food Color and Appearance; Aspen Publisher: Maryland, **1999**.
20. Judd, D. B.; Wyszecki, G. In Color in Business. Science and Industry; Wiley-Interscience: New York, **1975**.
21. Barham, P. J.; Keller, A.; Otun, E. L.; Holmes, P. A. *J. Mater. Sci.* **1984**, *19*, 2781.
22. ASTM. Standard test method for tensile properties of thin plastic sheeting. Standard D882 *Annual book of American standard testing* methods. American Society for Testing and Materials: Philadelphia, PA, **2010**.
23. Peterson, L.; Oksman, K. *Compos. Sci. Technol.* **2006**, *66*, 2187.
24. Zhan, M.; Wool, R. P. *Polym. Compos.* **2011**, 937.
25. Barone, J. R.; Schmidt, W. F.; Liebner, C. F. E. *J. Appl. Polym. Sci.* **2005**, *97*, 1644.
26. Cheng, S.; Lau, K.-T.; Liu, T.; Zhao, Y.; Lam, P.-M.; Yin, Y. *Compos. Part B: Eng.* **2009**, *40*, 650.
27. Prochon, M.; Janowska, G.; Przepiorkowska, A.; Kucharska-Jastrzabek, A. *J. Therm. Anal. Calorim.* **2012**, *109*, 1563.
28. Beall, G. W. New Conceptual Model for Interpreting Nanocomposite Behavior; In Polymer-Clay Nanocomposites; Pinnavaia, T. J.; Beall, G. W. Eds.; John Wiley & Sons Inc.: New York, **2000**; p 267–279.
29. Gunaratne, L. M. W. K.; Shanks, R. A. *Eur. Polym. J.* **2005**, *41*, 2980.
30. Sánchez-Garcia, M. D.; Lagarón, J. M. *J. Appl. Polym. Sci.* **2010**, *118*, 199.
31. Spiridon, I.; Paduraru, O. M.; Rudowski, M.; Kozlowski, M.; Darie, R. N. *Ind. Eng. Chem. Res.* **2012**, *51*, 7279.
32. Sanchez-Garcia, M. D.; Lopez-Rubio, A.; Lagaron, J. M. *Trends Food Sci. Tech.* **2010**, *21*, 528.
33. Corre, Y. M.; Bruzaud, S.; Audic, J. L.; Grohens Y. *Polym. Test.* **2012**, *31*, 226.
34. Sanchez-Garcia, M. D.; Lagaron, J. M. *J. Appl. Polym. Sci.* **2010**, *118*, 188.
35. Maxwell, J. C. In A Treatise on Electricity and Magnetism; Clarendon Press: Oxford, UK, **1881**; Vol. *I*, pp 435–449.
36. Fricke, H. *Phys. Rev.* **1924**, *24*, 575.
37. Paul, D. R.; Bucknall, C. B. Polymer Blends, Vol. *2*: Performance; Wiley InterScience: New York, **2000**.
38. Kit, K. M.; Schultz, J. M. Gohil, R. M. *Polym. Eng. Sci.* **1995**, *35*, 680.
39. Martínez-Sanz, M.; Lopez-Rubio, A.; Lagaron, J. *J. Appl. Polym. Sci.* **2012**, *128*, 2197.
40. Sanchez-Garcia, M. D.; Lagaron, J. M. *Cellulose* **2010**, *17*, 987.